Spring 2018

Differential Gene Expression in Response to Hypoxia and Acidosis in Chest Wall Deformities and Chondrosarcoma

Jamie L. Durbin
Old Dominion University, jamie_hynes@yahoo.com

DIFFERENTIAL GENE EXPRESSION IN RESPONSE TO HYPOXIA AND ACIDOSIS IN CHEST WALL DEFORMITIES AND CHONDROSARCOMA

by

Jamie L. Durbin

B.S. Biology May 2014, Old Dominion University

A Thesis Submitted to the Faculty of

Old Dominion University in Partial Fulfillment of the

Requirements of the Degree of

MASTER OF SCIENCE

BIOLOGY

OLD DOMINION UNIVERSITY
May 2018

Approved by:

Chris Osgood (Director)

Michael Stacey (Member)

Emilia Oleszak (Member)

ABSTRACT

DIFFERENTIAL GENE EXPRESSION IN RESPONSE TO HYPOXIA AND ACIDOSIS IN CHEST WALL DEFORMITIES AND CHONDROSARCOMA

Jamie L. Durbin
Old Dominion University, 2018
Director: Dr. Chris Osgood

The importance of understanding how costal cartilage chondrocytes respond to stimuli such as oxidative stress and low pH has been largely overlooked in studies involving tissue culturing due to major differences between oxygen and pH levels during incubation and the natural environment of hyaline cartilage. Hyaline cartilage is avascular and naturally hypoxic which subsequently leads to increased glycolytic metabolism and ultimately causes a decrease in extracellular pH. To examine how healthy costal cartilage responds to these extreme growth conditions, we examined responses in three hyaline cartilage diseases. Our ability to identify the disease mechanisms responsible for pectus excavatum, pectus carinatum, and chondrosarcoma are limited by our understanding of how these mechanisms operate. This study aimed to determine the roles of hypoxia and extracellular acidosis on the expression of genes related to the hypoxia response pathway in costal cartilage chondrocytes, two pectus chest wall deformities, and the hyaline cartilage producing cancer, chondrosarcoma. Cells isolated from costal cartilage were incubated under four experimental conditions, where cultures were subjected to 24 hours of either hypoxia (5% oxygen) or normoxia, and 60 seconds of acidic media (pH 5.5) or kept at neutral pH (pH 7.2) just prior to RNA extraction. Expression levels for 84 genes were tested by RT-qPCR to determine genes of interest within the hypoxia response pathway. Two genes, factor 3 *F3* and lysyl oxidase *LOX*, were chosen based on high fold change within the preliminary study; two replicate experiments were repeated for a total of 12 patient samples. Our analysis showed no significant change in any cell type compared to the control. However, the control and PC sample groups showed significant upregulation of both *F3* (Control, p=0.0001, PC, p=0.0026) and *LOX* (Control, p=0.0009, PC, p=0.0047) within the cell type in response to hypoxia, but PE and JJ012 samples showed no significant response. Low pH had no significant effect on expression levels in any cell type. Further study of how cellular response mechanisms to hypoxia and acidosis in healthy and diseased hyaline cartilage is required to fill knowledge gaps and create understanding for new therapies to treat pectus chest wall deformities or chondrosarcoma cancer.

This thesis is dedicated to those affected by pectus chest wall deformities and chondrosarcoma, with hope that my research may help lead to better understanding of these conditions.

ACKNOWLEDGMENTS

The completion of my degree was heavily dependent on the help and goodwill of many people in different aspects of my life. My primary advisor, Dr. Chris Osgood, and committee member, Dr. Emilia Oleszak, have been a wonderful source of motivation and constant line of support for me, and I will always be grateful for my time with them. I would also like to thank Dr. Mike Stacey for allowing me to perform my research in his lab and for answering my unending chain of emails. My mentor, Dr. Ralph Stevens, allowed me to teach many of his courses and helped me find my passion for teaching. Thank you to Dr. Patrick Sachs, Dr. Pete Mollica, Dr. Dave Gauthier, Dr. Nina Semenova, and Dr. Loree Heller for use of their equipment. A very special thank you to Hannah Aichelman and Courtney Klepac for their expertise in R. Lastly, I would like to thank my husband for his continuous love and support for my choice in career, and my friends and family for believing in me.

TABLE OF CONTENTS

Page

LIST OF TABLES vii

LIST OF FIGURES viii

Chapter 1. INTRODUCTION 1

1.1 Cartilage Biology 1
1.2 Chest Wall Deformities 4
1.3 Chondrosarcoma 5
1.4 Effects of Hypoxia and Acidosis 6
1.5 Genes of Interest 7
1.6 Hypotheses and Significance 8

2. METHODS 10

2.1 Sample Collection 10
2.2 Cell Isolation 10
2.3 Cell Culturing 10
2.4 RNA Extraction and Reverse Transcription 11
2.5 2.5 Array Plates 11
2.6 RT-qPCR 11
2.7 Data Analysis 12

3. RESULTS 14

3.1 Preliminary Data 14
3.2 Genes of Interest Selection 17
3.3 Acidosis is not a Significant Factor in *F3* Expression, but Acidosis Marginally Upregulated *LOX* Expression 17
3.4 *LOX* and *F3* Expression Levels are Upregulated in Response to Hypoxia in Control and Pectus Carinatum 20
3.5 Combined Chronic Hypoxia and Transient Acidosis Slightly Diminishes the Effects of Hypoxia 23
3.6 Gene Expression of *F3* and *LOX* Significantly Differs Between Cell Types 25
3.7 *F3* ANOVA 26
3.8 *LOX* ANOVA 29

Chapter 4. DISCUSSION 31

Chapter 5. CONCLUSION 35

REFERENCES 36

VITA 39

LIST OF TABLES

Table Page

1. RT^2 Profiler^{TM} PCR Array Human Hypoxia Signaling Pathway Plus Genes..... 13
2. Post-hoc Tukey's Test for Cell Type in *F3* 26
3. Post-hoc Tukey's Test for Cell Type in *LOX* 26
4. *F3* Three Factor ANOVA Results..... 27
5. Post-hoc Tukey's Test for Cell Type and Oxygen Levels in *F3* Expression 28
6. *LOX* Three Factor ANOVA Results..... 29
7. Post-hoc Tukey's Test for Cell Type and Oxygen Levels in *LOX* Expression 30

LIST OF FIGURES

Figure Page

1. Osmolarity Regulation in Hyaline Cartilage 2
2. Aggrecan Distribution in Costal Cartilage Cross-sections 3
3. Physical Manifestations of Pectus Chest Wall Deformities 4
4. Preliminary ASIC2 Protein Expression 14
5. Preliminary Calcium Transit Response to Extracellular Acidosis 15
6. Replicate Calcium Transit Data 16
7. Heat Map of Fold Change Data from Array Plates 19
8. Average *F3* Expression in Response to Acidosis 20
9. Average *LOX* Expression in Response to Acidosis 21
10. *LOX* Expression in Response to Hypoxia 22
11. *F3* Expression in Response to Hypoxia 23
12. *F3* Expression in Response to Combined Hypoxia and Acidosis Compared to Hypoxia Alone 24
13. *LOX* Expression in Response to Combined Hypoxia and Acidosis Compared to Hypoxia Alone 25
14. Acid-Sensitive Ion Channels in Rat Cardiomyocytes 33

CHAPTER 1

INTRODUCTION

1.1 Cartilage Biology

Hyaline cartilage is a specialized type of connective tissue that is located throughout the body including at the ends of bones and inside epiphyseal growth plates. Its function is to protect, lubricate, and cushion joints and produce bone through the process of endochondral ossification. Chondrocytes, the main cell type found within hyaline cartilage, reside in a collagenous matrix devoid of nerves, blood vessels, and lymphatics that gives cartilage the durability required to maintain healthy joints. Chondrocytes reside within lacunae, or pockets within the extracellular matrix, in small aggregates called isogenous groups. The extracellular matrix (ECM) has unique mechanical properties due to the presence of collagen, proteoglycans, and glycoproteins, which produce a negative charge and to achieve electroneutrality sodium ions are attracted into the tissue along with water. Aggrecan, an essential large aggregating proteoglycan (LAP), is responsible for the maintenance of osmolarity within the tissue. The proteoglycan is attached to a chain of hyaluronic acid by a link protein. Aggrecan contains three globular domains with keratan sulfate and chondroitin sulfate binding regions between the second and third globular domains (Figure 1). The sulfated regions create a negative charge surrounding the proteoglycan, which in turn attract sodium ions and water to the area (Kiani et al., 2002). Aggrecan localizes around isogenous groups of chondrocytes to create the unique, gel-like matrix near the cells. Previous studies from our lab show an increase in aggrecan localization surrounding chondrocytes from the periphery to the interior. Chondrocytes towards the periphery have less aggrecan in their territorial matrix compared to chondrocytes located in the interior of the cartilage (Figure 2) (Stacey et al., 2012). [1]

[1] This thesis is formatted for the journal *Cell.*

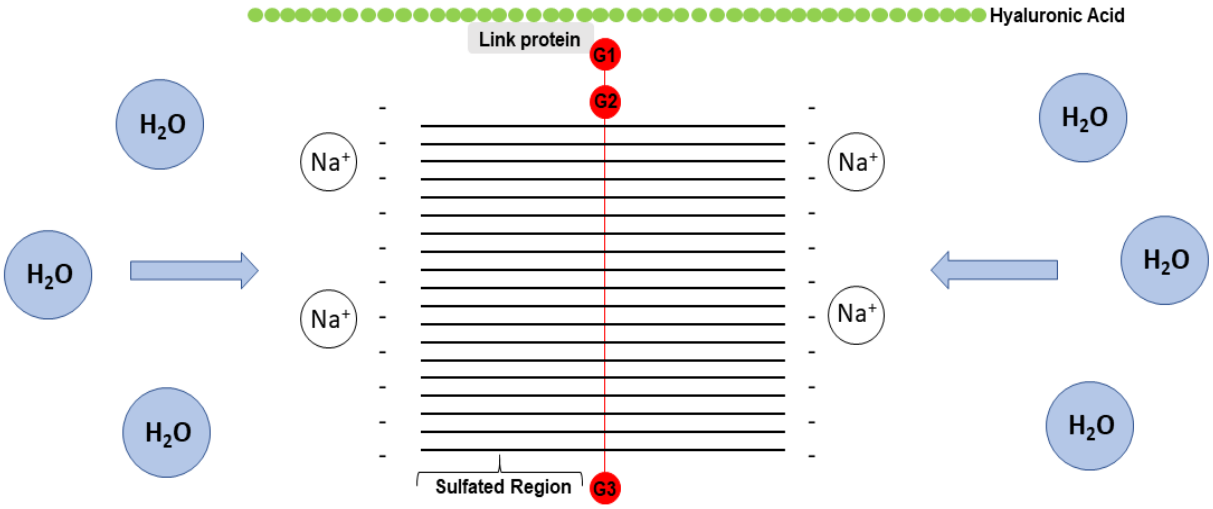

Figure 1. Osmolarity Regulation in Hyaline Cartilage
Aggrecan is connected to hyaluronic acid by a link protein and contains three globular domains with chondroitin sulfate and keratan sulfate between globular domains 2 and 3. The negative charge of the sulfated region attracts ions and water to the area.

Due to the size of the molecule, aggrecan is immobile in cartilage, but the surrounding area is dynamic (Kiani et al., 2002). Increased glycolytic metabolism due to hypoxia creates an accumulation of acid as a byproduct in the matrix surrounding the cell. The fluidity of the extracellular matrix causes transient flux in the charge and pH surrounding each cell as the protons, water, and other molecules fluctuate with movement. This fluctuation of the gel-like consistency within the matrix creates a unique environment of transient acidosis combined with hypoxia within costal cartilage (Dudhia, 2005; Kiani et al., 2002). Due to the transient change in pH combined with hypoxia, the cells in this study were exposed to brief acidosis to simulate the environment found within hyaline cartilage. High water content adds incompressibility and a small coefficient of friction to the tissue for smooth movement of joints and cushion for bones from the effects of gravity in areas such as the knee. While, a strong meshwork of cross-linked collagen fibers allows for flexibility as well as strength (Alice et al., 2009). This study looks at a specific location of hyaline cartilage, costal cartilage, and a hyaline cartilage producing cancer, chondrosarcoma. Costal cartilage is comprised of cords of hyaline cartilage that connect the ribs to the sternum and help provide a rigid yet flexible cage to protect our vital organs within the thoracic cavity whilst allowing for chest expansion during respiration.

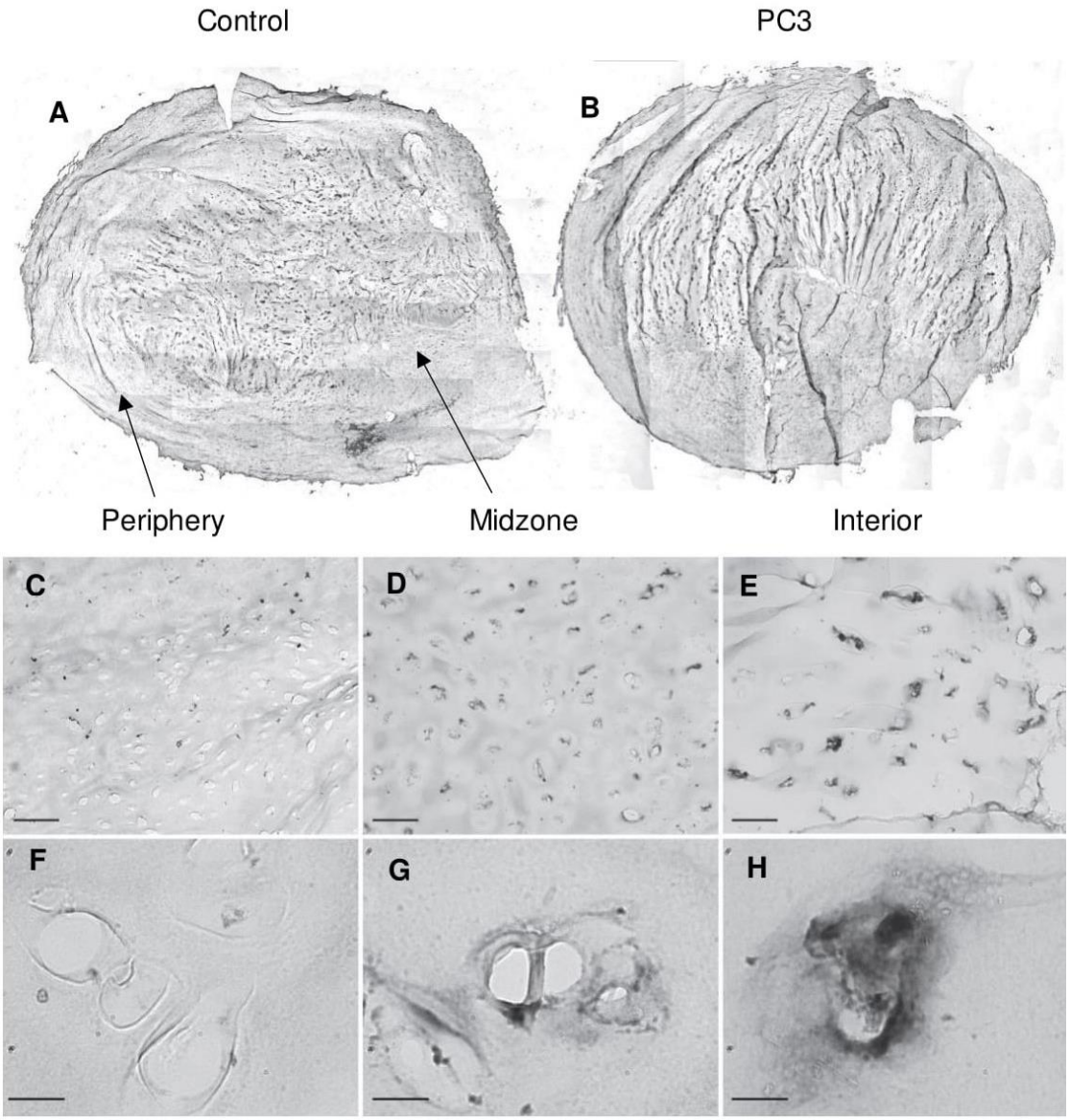

Figure 2. **Aggrecan Distribution in Costal Cartilage Cross-sections**
This figure demonstrates the localization of aggrecan in the extracellular matrix by immunohistochemistry (Scale bars = 10 μm). A) Distribution of aggrecan in whole Control section. B) Distribution of aggrecan in whole PC3 (pectus carinatum) section. C–E) Distribution of aggrecan in control at 10x magnification from C) periphery, D) midzone, and E) interior regions. Scale bars, 100 μm. F–H) Distribution of aggrecan in control at 100x magnification from F) periphery, G) midzone, and H) interior regions. Localization of aggrecan increases around each lacuna in the interior compared to the periphery (Stacey et al., 2012).

1.2 Chest Wall Deformities

Pectus chest wall deformities are characterized by sternal displacement due to abnormal growth of costal cartilage during development. The two most common forms of pectus deformities are pectus excavatum (PE), also known as funnel chest, and pectus carinatum (PC), also known as pigeon chest (Figure 3). The more common of the two, PE, is clinically presented in 1 out of every 500 live births presenting as a conical depression around the sternum and costal cartilage (Dean et al., 2012). Whereas PE patients have inward growth of costal cartilage, PC patients display outward growth of the sternum and associated costal cartilages. These diseases mainly occur at times of growth spurts during adolescence and affect males more often than females in a ratio of 4:1 in PE and 3:1 in PC (Williams and Crabbe, 2003). Treatment and repair for these deformities is usually done through surgical intervention. The Nuss procedure is a minimally invasive pectus repair used to correct the sternal position in PE patients (Nuss and Kelly, 2010), while the Ravitch procedure is used to correct the outward sternal position in PC patients.

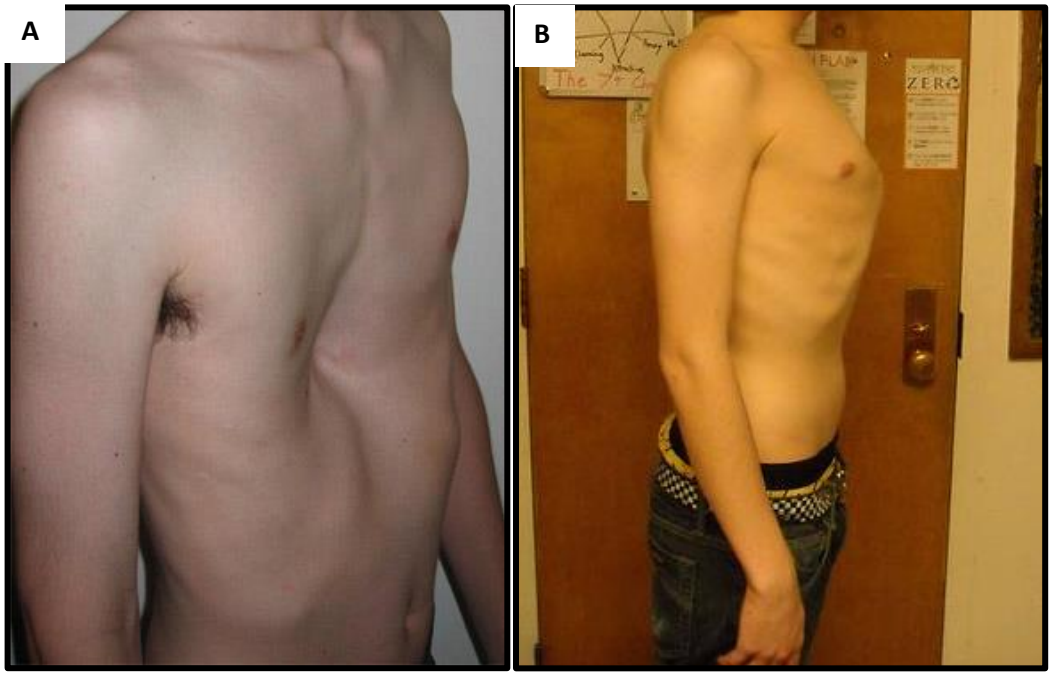

Figure 3. Physical Manifestations of Pectus Chest Wall Deformities
Chest of a male with (A) pectus excavatum and (B) pectus carinatum (Wikipedia, 2018a, b).

Other than surgical intervention, physiotherapy techniques such as encouraging good posture have not shown any reliable evidence in treating pectus deformities (Williams and Crabbe, 2003). Patients with PE and PC usually experience issues with respiration and cardiac abnormalities due to the shape of the chest cavity (Koumbourlis and Stolar, 2004). The cause of this abnormal growth has eluded scientists since its first description in 1594. Associated diseases such as Marfan's syndrome, Ehlers-Danlos syndrome, and scoliosis are often found in comorbidity with pectus deformities which only adds to the difficulty in pinning down the cause behind pectus diseases (Goretsky et al., 2004). Recent work in our lab has identified a unique 'nanostraw-like' structures that run the length of the costal cartilage (Stacey et al., 2012) that contributes to sustaining the mechanical properties of this tissue (Huwe et al., 2017a), although correlation of these disorders to matrix abnormalities has not been possible (Asmar et al., 2015; Shen et al., 2018; Stacey et al., 2013). Although the pathogenesis of pectus deformations is unclear, a case of familial pectus carinatum has been recorded in our lab and other familial incidences of PE and PC have been recorded throughout the literature, suggesting a heritable form of PC (Creswick et al., 2006; Horth et al., 2012). The genes responsible for this hereditary nature are unknown and further investigation into disease mechanism is required.

1.3 Chondrosarcoma

Chondrosarcoma is a form of cartilage-producing cancer where hyaline cartilage invades the bone and soft tissues. Even though it is the second most common form of bone cancer, chondrosarcoma is quite rare. Most cases develop de novo, but secondary chondrosarcoma can be caused by osteochondroma, a benign precursor lesion on the bone (Jeong and Kim, 2018). Most chondrosarcoma patients exhibit slow growth with rare metastases and usually have a good prognosis with proper tumor excision, but high-grade chondrosarcoma is much more aggressive. Literature for high-grade chondrosarcoma disease etiology is sparse due to its low frequency but has become a hot spot for research due to its highly metastatic and highly proliferative pathology. These cancerous cells are resistant to chemotherapy and radiation, which leaves surgical intervention as the main source of treatment. However, patients with high-grade chondrosarcoma tend to develop local recurrence and distant metastasis after surgical intervention (Jeong and Kim, 2018) with poor outcomes.

The extracellular environment within these solid tumors is comprised of hyaline cartilage matrix and thus provides hypoxic and acidic stress on the cancer cells comparable to that in other

types of hyaline cartilage. As shown below, our preliminary data show downregulation of *Sox5* and *Sox9* genes and upregulation of *OGR1* in response to low pH. When exposed to growth media at pH 5.5, acid-sensitive ion channels open to transit calcium into the cytoplasm from the extracellular environment and the endoplasmic reticulum. A recent study on cardiomyocytes shows that calcium release causes an upregulation of the hypoxia response and HIF-1A. The hypoxia response activates SOX5 and SOX9 causing extracellular matrix remodeling (Hu et al., 2017). Using these data, we will incorporate chondrosarcoma cell line, JJ012, as a separate experimental group to determine the role of acidosis and hypoxia in chondrosarcoma disease etiology.

1.4 Effects of Hypoxia and Acidosis

The canonical hypoxia response in cells induces a family of transcription factors known as hypoxia-inducible factors (HIFs) to regulate expression of a variety of genes responsible for multiple physiological processes and the response varies among cell types. The HIF-1 (Hypoxia Inducible Factor 1) protein is the major regulator for oxygen homeostasis in human tissues, although its complete pathway is not fully understood. Downstream effects from target genes of HIF-1α, the alpha subunit of the HIF protein, regulate physiological responses to combat hypoxia by increasing oxygen delivery through processes such as angiogenesis and/or reducing oxygen consumption through promotion of anaerobic metabolism (Kanehisa et al., 2017; Kanehisa and Goto, 2000; Kanehisa et al., 2016). Due to continuous hypoxia, as demonstrated in chondrocytes, nitric oxide molecules accumulate within the mitochondria as byproducts of metabolism, which can initiate apoptosis if not properly disposed of in a timely manner (Zhong et al., 2008).

In response to hypoxia, cells increase anaerobic metabolism which subsequently leads to an excess of lactic acid accumulation as a byproduct of glycolytic metabolism (Kanehisa et al., 2017; Kanehisa and Goto, 2000; Kanehisa et al., 2016). This increase in acid in the extracellular matrix creates transient acidosis as the ECM changes with movement and compression of the tissue. Cellular response to acidosis in chondrocytes in not well understood, but studies suggest acid-sensitive ion channels (ASICs) and intracellular calcium transit may cause changes in gene transcription. Ovarian cancer G protein-coupled receptor 1 (OGR1) has been shown to be a receptor for protons and is involved in acid-induced apoptosis in endplate chondrocytes in intervertebral discs (Yuan et al., 2014). When protons bind to OGR1, calcium accumulates in the cytoplasm from intracellular stores and initiates apoptosis pathways. The mechanisms

present in this study of intervertebral discs composed of fibrocartilage offer insight comparable to acidosis response in hyaline cartilage.

The molecular mechanisms and gene expression changes in response to the extracellular environment in pectus deformities are unknown. Chondrocytes in costal cartilage are responsible for forming their extracellular matrix in an avascular and low pH environment. These cells operate under chronic hypoxia (low oxygen supply) and transient acidosis (low pH) due to the avascular nature of cartilage and glycolytic metabolism resulting in acid production as a by-product. The effects of both hypoxia and acidosis together are not fully understood, but models within solid breast tumor environments found hypoxia and lactic acidosis synergistically upregulate the unfolded protein response genes, increase inflammatory response genes, and inhibit canonical hypoxia response pathways. In this model, hypoxia regulator proteins such as HIF-1α were upregulated under hypoxic conditions. However, the tumor cells downregulated transcription of the *HIF-1α* gene in the presence of combined mild extracellular lactic acidosis and hypoxia (Tang et al., 2012).

1.5 Genes of Interest

The response of chondrocytes to combined hypoxia and acidosis is largely unknown and is an important gap in knowledge with respect to their biology and function. Hypoxia related response can be measured by changes in gene expression, however, much of the work on gene expression has been performed on other cell types where expression may not be relevant to chondrocyte biology. Conversely, genes otherwise not known to be expressed in chondrocytes may be identified that would open the question as to why these genes are expressed and what is their function, thus opening new avenues of research in chondrocyte biology.

Gene array plates offer such an approach, but as described above, the function of the genes on these plates tend to be related to angiogenesis, coagulation, metabolism and apoptosis. Through literature searches, we identified a paper by Zhong et al. and another by Huwe et al. describing expression of angiogenesis and coagulation factor related genes in chondrocytes.

Also named tissue factor, thromboplastin, and coagulation factor III, F3 is a cell surface glycoprotein encoded by the *F3* gene. The *F3* gene, is located on the small arm of chromosome 1 (1p21.3) and is 12,682 bases in size. The F3 protein is found throughout the body and functions as a high- affinity receptor for factor VII to create a complex that catalyzes the activation of the blood-clotting cascade through proteolytic activity. The F3/Factor VII complex cleaves the inactive, immature prothrombin protein into active, mature form thrombin

(Genecards.org, 2018a). Thrombin, also known as coagulation factor II/F2, activation functions in later stages of clotting by enzymatically crosslinking fibrin to form a fibrin scaffold mesh around the platelet plug to hold it in place (Licari and Kovacic, 2009). Other possible functions for F2 and F3 proteins in costal cartilage are not well known, but some literature suggests possibilities in endochondral bone formation. The thrombin peptide TP508 prevented nitric oxide (NO) mediated apoptosis in chondrocytes isolated from cartilage in the process of endochondral ossification in the epiphyseal growth plate. In the growth plate, increased inorganic phosphate (Pi) and NO accumulated in the cell due to increased nitric oxide synthase (iNOS) activity, and initiated apoptosis. Thrombin peptide TP508 prevented cell death through inhibition of iNOS dependent NO production. Other observed effects include increased extracellular matrix production, and maintained chondrocyte proliferation while the alkaline phosphatase activity, which is essential for proliferation, was reduced (Zhong et al., 2008).

Due to the scaffolding properties of fibrin exhibited during blood clot formation, fibrin-based scaffolds within a gel are currently being examined as a biomaterial used to initiate wound healing at injury sites in articular and fibrocartilage (de Barros et al., 2016). In context to our study, blood clotting is not a common occurrence in costal cartilage due to the avascular nature of hyaline cartilage, however alternative functions of these genes related to chondrocyte function may be possible.

The lysyl oxidase gene, *LOX*, is a protein coding gene located on the long arm of chromosome 5 (5q23.1) and is 15,166 bases in size. The lysyl oxidase family of enzymes consists of many variants produced through alternative splicing, but only one leads to a mature enzyme (Genecards.org, 2018b). The mature LOX enzyme is a copper-dependent amine oxidase which crosslinks collagen and elastin fibers. Proper collagen crosslinking is essential for cartilage survival when the tissue is continuously subjected to harsh environments. A study from 2017 using costal chondrocytes to engineer articular cartilage in an ovine model indicated that developing neocartilage treated with a mixture of lysyl oxidase-like protein 2 (LOXL2), TGF-B1, and cABC significantly improved the tensile strength, possibly due in part to proper collagen crosslinking (Huwe et al., 2017b). This study examined expression of *F3* and *LOX* genes in non-differentiating chondrocytes isolated from costal cartilage in response to oxidative stress and extracellular acidosis. The significance of this data will help to determine how chondrocytes function in an environment closer to hyaline cartilage inside the body.

1.6 Hypotheses and Significance

Most studies involving cultured chondrocytes are conducted under normoxia and neutral pH levels even though these experimental conditions are not comparable to the *in vivo* environment. This study objective is to determine that cultured chondrocytes initiate a hypoxia response to hypoxic conditions that may be modulated by acidic stressors on a transcriptional level. We aim to determine expression levels of genes *F3* and *LOX* in chondrocytes in combined chronic hypoxia and transient acidosis between and among normal costal cartilage, pectus excavatum, pectus carinatum, and chondrosarcoma cell line, JJ012. The roles of F3 and LOX in costal cartilage chondrocytes is not well understood, but studies in other types of cartilage suggest F3 function in the prevention of NO mediated apoptosis, and LOX function in enzymatic crosslinking of collagen fibers. Based on previous literature, **I hypothesize that *F3* mRNA levels would be upregulated in cultures grown under hypoxic and acidic conditions to compensate for elevated levels of nitric oxide.** LOX enzymes crosslink collagen fibers to increase the tensile strength of cartilage. In surgical repair for pectus deformities, the cartilage has been reported to be more malleable and not properly formed, and chondrosarcoma tumors produce hyaline cartilage within the tumor environment. Due to this possible connection, **I hypothesize that *LOX* mRNA levels would be downregulated in patients with pectus excavatum, pectus carinatum, and chondrosarcoma compared to control costal cartilage due to malformation of the cartilage.** The disease mechanisms for pectus chest wall deformities remain poorly understood and information about the mechanisms involved with oxygen homeostasis in costal cartilage chondrocytes is incomplete. Further evaluation of environmental factors such as acidosis and hypoxia will allow a better understanding of cellular responses in pectus deformities and in chondrosarcoma disease etiology.

CHAPTER 2

MATERIALS AND METHODS

2.1 Sample Collection

Human costal cartilage was obtained from 3 patients with pectus carinatum and 3 patients with pectus excavatum all severe enough to warrant surgical repair. All samples were collected with informed consent and Institutional Review Board (IRB) approval IRB# 17-185 and all guidelines were followed by the Institutional Biosafety Committee (IBC) IBC# 18-007 from Old Dominion University and Eastern Virginia Medical School. The IRB protocol currently prevents disclosure of many clinical features and thus close correlation of clinical phenotype with expression is not possible.

2.2 Cell Isolation

Age matched costal cartilage samples were obtained from the Children's Hospital of the King's Daughters in Norfolk, Virginia. Chondrocytes were isolated from tissue through enzyme mediated collagen digestion. Costal cartilage specimens were cut into pieces a few millimeters in size and washed with 20mL PBS. Next, the cartilage was transferred to a 50mL conical tube with 10mL PBS with 10% collagenase added and placed in an Excella E24 incubator shaker (New Brunswick Scientific, Edison, New Jersey) at 37ºC and 200 RPM for 4 hours to isolate cells from the matrix. Cells were pelleted at 200g and suspended in fresh growth medium and expanded briefly in tissue culture. Cells were then frozen at -80ºC in DMEM supplemented with 10% DMSO to prevent crystallization and stored in liquid nitrogen until needed.

2.3 Cell Culturing

Cultures with low passage numbers were expanded in flasks with Dulbecco's Modified Eagle Medium (DMEM) supplemented with 10% Chondrocyte Growth Supplement and 1% Streptomycin/Penicillin until proper cell density was achieved. Cells were then transferred to conical tubes and, to maintain a differentiated phenotype, grown in 3D pellet cultures at a seeding density of 10^6 cells per culture. Each sample was split into 4 experimental groups and grown under separate conditions in either normoxia at pH 7, normoxia at pH5.5, hypoxia at pH 7, or hypoxia a pH 5.5 for 24 hours. Hypoxic cultures were grown in a separate incubator at 95% N_2 and 5% O_2 at 37ºC and normoxia cultures were grown at 37ºC with 5% CO_2. All cultures subjected to lower pH were incubated with media at pH 5.5 for 60 seconds just prior to RNA extraction. All media used in hypoxic environments was degassed for 24 hours in vacuum

chamber (Scienceware Dessicator, Bel-Art Products, Pequannock, New Jersey) and equilibrated overnight in the hypoxia incubator. All 4 disease cases were grown with 3 age matched patient samples for each cell type in each experimental condition for a total of 48 cell cultures.

2.4 RNA Extraction and Reverse Transcription

After growing in culture under experimental conditions for 24 hours, the cells were lysed in culture by adding 350µL of Trizol directly to the well. After 10 minutes of incubation at room temperature for 10 minutes, equal volume of 100% ethanol was added to the lysate. Total RNA was extracted using the Direct-zol™ RNA MiniPrep Kit (Zymo Research Corp, Irvine, California) as suggested by the manufacturer and tested for concentration and quality using a Nanovue Plus Spectrophotometer (GE Healthcare, Little Chalfont, UK). The RNA was then converted to complementary DNA (cDNA) using the RT First Strand Kit (Qiagen, Valencia, California) as suggested by the manufacturer and tested for concentration and quality using the Nanovue.

2.5 Array plates

Genes of Interest for the replicate experiments were chosen from 84 genes that are represented on the Profiler™ PCR Array Human Hypoxia Signaling Pathway Plus (Qiagen, Valencia, California) (Table 1). A full array plate was run for one patient sample from all four cell types, grown under all four experimental conditions. The array plates were run on a BioRad CFX96 thermalcycler (BioRad, Hercules, California) utilizing RT^2 SYBR Green qPCR Mastermix (Qiagen, Valencia, California) detection. A stock of 1350µL SYBR mastermix, 1248µL DNA grade water, and 102µL cDNA templates were made and 25µL of stock was added to each well of the array plate (primers are already in wells). After an initial denaturation step at 95ºC for 10 minutes, the cDNA products were amplified for 40 cycles of 95ºC for 15 seconds to denature and 60ºC for 60 seconds to extend and anneal. A melt curve was performed at the end of all 40 cycles from 65ºC to 95ºC in 0.2ºC increments to determine specificity of the amplicons. GAPDH was excluded as a housekeeping gene from analysis due to its role in the HIFα pathway response to hypoxia.

2.6 RT-qPCR

After we determined our genes of interest from the array plates, we replicated the RT-qPCR expression experiments focusing on genes *LOX* and *F3*. Human primer oligos for *F3* and *LOX* (Qiagen, Valencia, California) were utilized instead of full array plates to reduce cost and time.

The PCR mastermix consisted of 12.5µL SYBR Green Mastermix, 10.5µL DNA grade water, 1µL primer, and 200ng cDNA template (typically 1 µL through RT first strand kit). In each well, 25µL of the mastermix was added and each sample was run in triplicate using the same cycling protocol as the array plates. After an initial denaturation step at 95ºC for 10 minutes, the cDNA products were amplified for 40 cycles of 95ºC for 15 seconds to denature and 60ºC for 60 seconds to extend and anneal. A melt curve was performed at the end of all 40 cycles from 65ºC to 95ºC in 0.2ºC increments to determine specificity of the amplicons. Genes of interest were compared to a housekeeping gene, ACTB (Beta Actin) (Qiagen, Valencia, California). GAPDH and 18SrRNA were excluded from our housekeeping genes due to their active involvement with the hypoxia response. Primer sequences are proprietary, and thus the RT-qPCR reactions were run according to manufacturer standards. Melt curves were performed to assure specificity of the amplicons. All melt curve peaks revealed no significant variation across all samples and genes.

2.7 Data Analysis

Gene expression data from the array plates was analyzed using the ΔΔCq method to determine fold change while examining genes of interest. Once these genes were determined, a Three Factor Analysis of Variance (ANOVA) and post-hoc Tukey's Tests (Confidence levels = 0.95) were performed on replicate Cq values using RStudio software to determine significant change in expression between samples (CoreTeam, 2013). An error statistic was added to account for patient variability, which was not a significant factor to the analysis. The threshold of significance was set as $P<0.05$.

Table 1. RT^2 Profiler^{TM} PCR Array Human Hypoxia Signaling Pathway Plus Genes

Function Group	Genes
HIF1 & Co-Transcription Factors	*ARNT, COPS5, HIF1A, HIF1AN, HIF3A, HNF4A, NCOA1, PER1*
Other HIF1 Interactors	*APEX1, EGLN1, EGLN2, NFKB1, P4HA1, P4HB, TP53 (p53)*
Angiogenesis	*ADORA2B, ANGPTL4, ANXA2, BTG1, EGR1, EDN1, EPO, F3, GPI, HMOX1, JMJD6, LOX, MMP9, PGF, PLAU (UPA), SERPINE1 (PAI-1), VEGFA*
Coagulation	*ALDOA, ANXA2, F10, F3, PLAU (UPA), SERPINE1 (PAI-1), SLC16A3*
DNA Damage & Repair	*ATR, MIF, NDRG1, RUVBL2*
Metabolism	*ALDOA, DDIT4 (REDD1), ENO1, ERO1L (ERO1L), GBE1, GPI, GYS1, HK2, LDHA, PDK1, PFKFB3, PFKFB4, PFKL, PFKP, PGAM1, PGK1, PKM, SLC2A1, SLC2A3, TPI1*
Regulation of Apoptosis	*ADM, BNIP3, BNIP3L, BTG1, DDIT4 (REDD1), IER3, MIF, NOS3 (eNOS), PIM1*
Regulation of Cell Proliferation	*ADM, BTG1, BLM, CCNG2, EGR1, IGFBP3, MET, MIF, MXI1, NAMPT, NOS3 (eNOS), ODC1, PGF, PIM1, TXNIP*
Transcription Factors	*BHLHE40 (DEC1), FOS, RBPJ (RBPSUH), USF2*
Transporters, Channels, & Receptors	*SLC2A1, SLC2A3, SLC16A3, TFRC, VDAC1*
Other Hypoxia Responsive Genes	*ANKRD37, CA9, CTSA, DNAJC5, EIF4EBP1 (4E-BP1), LGALS3, MAP3K1 (MEKK1)*
Housekeeping Genes	*ACTB, B2M, GAPDH, HPRT1, RPLP0*

These genes were tested in one patient sample of each cell type in each of the four experimental conditions. Genes are grouped by their function in the hypoxia response pathway.

CHAPTER 3

RESULTS

3.1 Preliminary Data

Given a mechanistic link between hypoxia and acidosis, connections between these stresses have been found. We have identified acid sensitive ion channels (ASICs) present in costal cartilage chondrocytes that may be compromised under hypoxic conditions (Asmar et al., 2016). Acid sensitive ion channels elicit intracellular calcium release in response to moderately low pH (pH 5.5) which can lead to tissue damage. Our preliminary data suggests that ASIC2 protein expression may be downregulated in PC samples when compared to healthy costal cartilage (Figure 4).

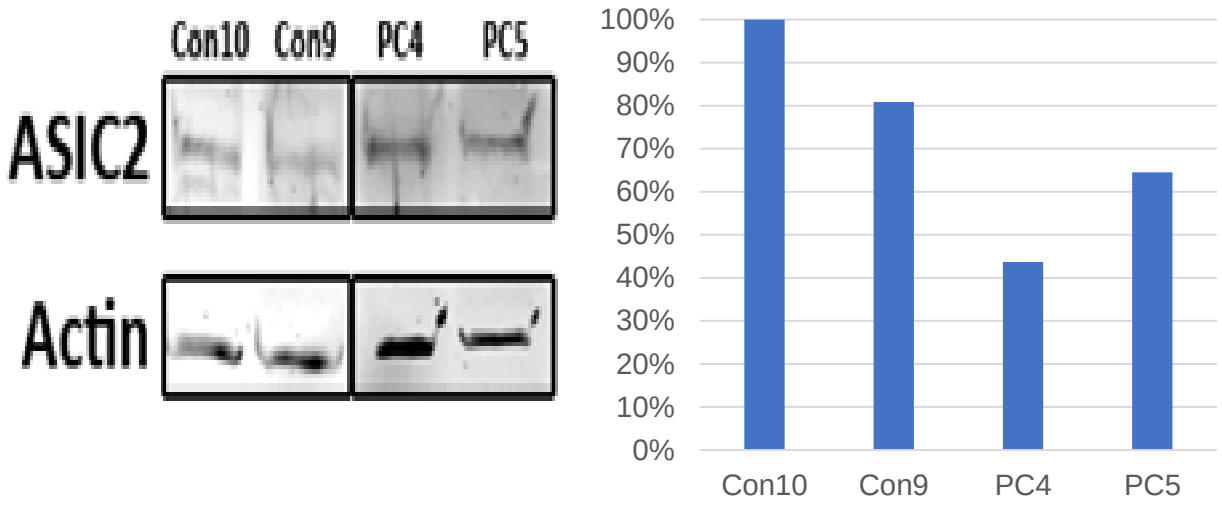

Figure 4. Preliminary ASIC2 Protein Expression
Western blot images suggest a decrease in the presence of Acid Sensitive Ion Channel 2 (ASIC2) in cells derived from costal cartilage in two patient samples who underwent surgical repair for pectus carinatum (PC4 and PC5) compared to healthy costal cartilage chondrocytes (Con10 and Con9). However, the results from this experiment are inconclusive and require further inquiry.

The mechanisms for calcium transit in chondrocytes are unknown, but we have identified the presence of ovarian cancer G protein-coupled receptor 1 (OGR1) along with other genes that may be responsible for irregular calcium transit in pectus deformities and chondrosarcoma. In chondrocytes, OGR1 was recently identified to be a receptor for protons when exposed to low pH in the extracellular matrix (Yuan et al., 2014). This binding event stimulates intracellular calcium release from internal stores, primarily the endoplasmic reticulum, leading to apoptosis and activation of calcium-sensitive proteases through downstream signaling (Yuan et al., 2014). The effects of acidosis and hypoxia on acid sensitive channels in pectus deformities and chondrosarcoma have yet to be identified. Preliminary data from our lab shows calcium transit in PC samples is delayed compared to healthy chondrocytes when subjected to low pH and PC samples' responses of calcium release dulls over time (Figure 5 and 6).

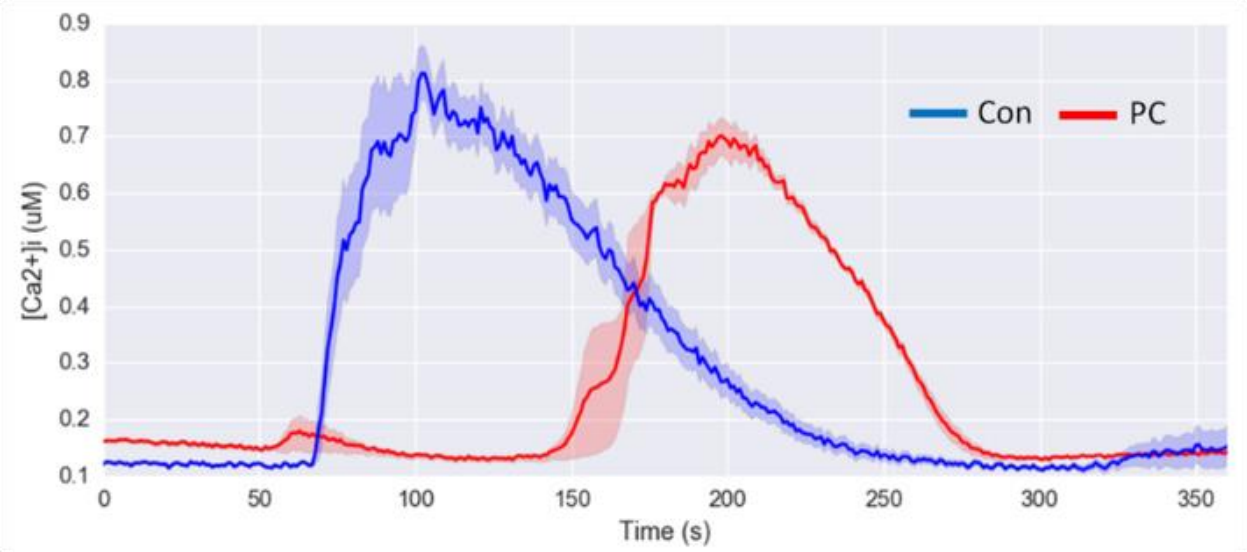

Figure 5. Preliminary Calcium Transit Response to Extracellular Acidosis
Single cells mounted to a cover slip were stained with Fura2-AM dye to observe a real-time response to calcium release. The cells were washed with a low pH media in a vacuum chamber mounted to a microscope to elicit intracellular calcium release from internal stores. The ratiometric Fura2-AM dye fluoresces in the presence of intracellular calcium and was recorded in real-time through fluorescence intensity and video to determine the relative amount of calcium released. This graph shows a control costal chondrocyte (Con, blue) that released calcium around 60 seconds after exposure to media at pH 5.5, while the pectus carinatum sample (PC, red) had a delayed and less intense response at approximately 150 seconds after exposure.

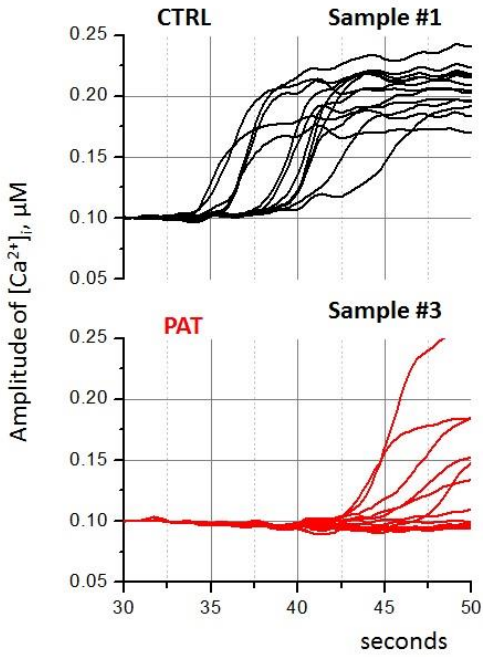

Figure 6. Replicate Calcium Transit Data
Replicate experiments performed by Dr. Iurii Semenov from the Frank Reidy Center for Bioelectrics at Old Dominion University from the initial calcium experiment in Figure 3 indicate that the control chondrocytes (CTRL, black) have a high variation in response, but still tend to have a faster and more intense response compared to the pectus carinatum cells (PAT, red).

Our preliminary data from the calcium transit studies show that extracellular calcium at moderately low levels could have a negative effect on ion transport in chondrocytes. However, the response to simultaneous mild extracellular acidosis at pH 6.5 and hypoxia has been shown to have morphological and possible protective effects on mitochondrial function in cortical neurons (Khacho et al., 2014). The phenomenon of mitochondrial fragmentation or mitochondrial fission is a dominant phenotype of cells responding to oxygen stressors. Cortical neurons grown at 1% oxygen levels displayed significant mitochondrial fission at neutral pH (pH 7.2) and severe acidosis (pH 6.0) but had only slightly elongated mitochondria with mild extracellular acidosis (pH 6.5). When observed over time, the mitochondria from cells exposed to mild acidosis began to reverse the damage caused and mitochondrial fusion began. The protective effect for mitochondrial morphology may be an important pathway for preventing cell

death under severe hypoxia in stroke victims. The response to acidosis and hypoxia in cartilage is not well documented, and further studies are required to determine the signaling pathways involved in response to these stressors (Khacho et al., 2014).

3.2 Genes of Interest Selection

Genes of interest were selected through analysis of the array plate data. Data visualization through production of a heat map created with R software allowed us to view fold change data between and among each cell type and treatment group as a color gradient (Figure 7). The darker colors represent the samples with the highest negative fold change values and the lighter colors represent the samples with the highest positive fold change values. We chose our genes of interest, Factor 3 (*F3*) and Lysyl Oxidase (*LOX*), based on the most consistent values with high fold change.

3.3 Acidosis is not a Significant Factor in F3 Expression, but Acidosis Marginally Upregulated LOX Expression

F3 expression levels overall were not significantly different between pH levels 5.5 and 7 ($p=0.08389$) across all treatment groups (Figure 8). However, pH alone had a marginally significant effect ($p=0.0368$) on *LOX* expression, but none of the interaction factors that included pH were significant. *LOX* expression levels were lower in the samples grown in normoxia at pH 5.5 than any other condition. Acidic conditions alone downregulated gene expression of *LOX* in control and JJ012 compared to neutral pH in normoxic conditions. However, the pectus samples showed little change in *LOX* expression due to a decrease in extracellular pH without the presence of hypoxia.

Figure 7. Heat Map of Fold Change Data from Array Plates

Fold change data from hypoxia array plates from four patient samples is visually represented by color. Light colors equal positive fold change and dark colors equal negative fold change for each of the 84 genes tested. Each comparison of treatment groups is represented on the x-axis and each gene tested is represented on the y-axis. Each patient sample is represented by a either C=control, PC=pectus carinatum, PE=pectus excavatum, JJ012=chondrosarcoma and a number. Legend: N=normoxia, H=hypoxia, 7=pH 7, 5.5=pH 5.5


CA9
SLC2A1
GYS1
BNIP3
PFKFB4
NDRG1
PDK1
FAM162A
PGK1
JMJD6
ERO1L
EIF4EBP1
VDAC1
SLC2A3
IER3
EGLN1
PFKP
RBPJ
P4HA1
MXI1
LDHA
RPLP0
BNIP3L
ANXA2
COPS5
LGALS3
ANKRD37
NAMPT
GBE1
CCNG2
TPI1
PFKL
PFKFB3
GAPDH
ALDOA
BHLHE40
P4HB
PER1
SLC16A3
TXNIP
MET
ODC1
TP53
ACTB
ENO1
EDN1
HPRT1
RUVBL2
MIF
F10
PGF
PKM2
DNAJC5
CTSA
USF2
HIF1AN
APEX1
NFKB1
EGLN2
ATR
FOS
GPI
MAP3K1
EPO
MMP9
NOS3
HIF3A
ARNT
NCOA1
B2M
HIF1A
ANGPTL4
VEGFA
SERPINE1
IGFBP3
ADORA2B
HK2
ALDOC
DDIT4
PIM1
LOX
HMOX1
BLM
TFRC
EGR1
PLAU
F3
ADM
HNF4A
C02H7_T03H7
T03H7_T03H5.5
C02H5.5_JJ012H5.5
C02N7_JJ012N7
C02N5.5_JJ012N5.5
C02H7_JJ012H7
T03N7_T03H7
JJ012N7_JJ012N5.5
PC6N7_PC6N5.5
JJ012N7_JJ012H7
C02N7_C02N5.5
C02N7_PC6N7
C02H7_PC6H7
C02H7_C02H5.5
C02H5.5_T03H5.5
C02N7_T03N7
C02N5.5_T03N5.5
JJ012H7_JJ012H5.5
C02N5.5_PC6N5.5
C02H5.5_PC6H5.5
PC6H7_PC6H5.5
T03N7_T03N5.5
JJ012N5.5_JJ012H5.5
PC6N7_PC6H7
C02N7_C02H7
C02N5.5_C02H5.5
T03N5.5_T03H5.5
PC6N5.5_PC6H5.5

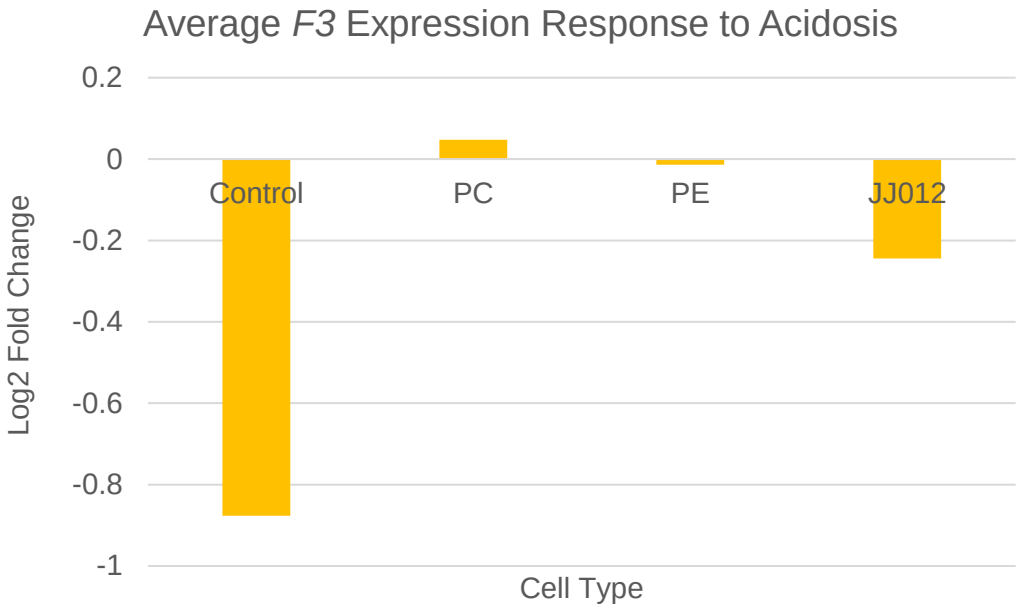

Figure 8. Average *F3* Expression in Response to Acidosis
Log2 fold change for *F3* expression was averaged across three patient samples per cell type to determine that all fold change was less than 1-fold difference across all cell types. All cultures for this figure were exposed to transient acidosis at pH 5.5 for 60 seconds prior to RNA extraction to elicit a response.

Combined acidosis and hypoxia appears to slightly increase *LOX* expression in control and PC samples, but the combination induced little change in expression in JJ012 and PE samples. Overall, hypoxia and acidosis, either combined or isolated, had little effect on *LOX* expression in the PE samples (Figure 9).

3.4 LOX and F3 Expression Levels are Upregulated in Response to Hypoxia in Control and Pectus Carinatum

Overall, hypoxic conditions had a significant effect *(LOX* p=1.81e-06, *F3* p=2.02e-06) on expression levels over all samples in all treatment groups for both *LOX* and *F3*. Genes *LOX* and *F3* were significantly upregulated in response to hypoxia within samples from the control and PC groups compared to normoxia. On average, control samples grown under hypoxic conditions at neutral pH upregulated expression of *LOX* by 7.9-fold whereas PC samples grown under hypoxia upregulated *LOX* by 19.6-fold on average (Figure 10). Patient variability was not

a significant factor in this analysis but shown in the figure, variation in expression does occur. Beta Actin, *ACTB*, was used as the housekeeping gene during analysis. On average, control samples grown under hypoxic conditions at neutral pH upregulated expression of *F3* expression by 28.4-fold and PC samples grown in hypoxia upregulated *F3* by 9.5-fold (Figure 11).

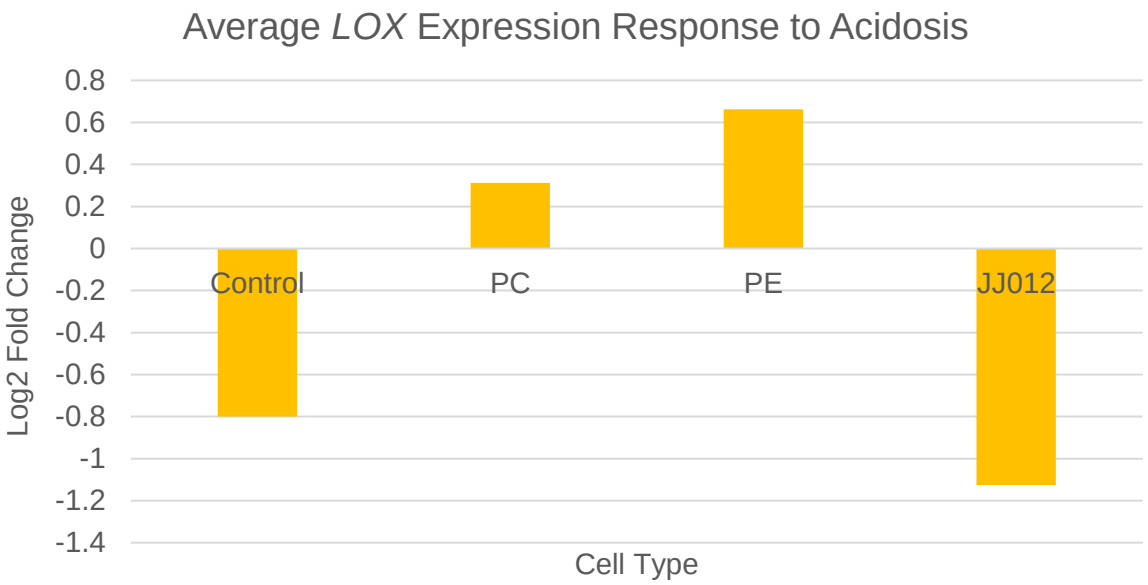

Figure 9. Average *LOX* Expression in Response to Acidosis
Log2 fold change for *LOX* expression was averaged across three patient samples per cell type to determine that all fold change was less than 1.2-fold difference across all cell types. All cultures for this figure were exposed to transient acidosis at pH 5.5 for 60 seconds prior to RNA extraction to elicit a response.

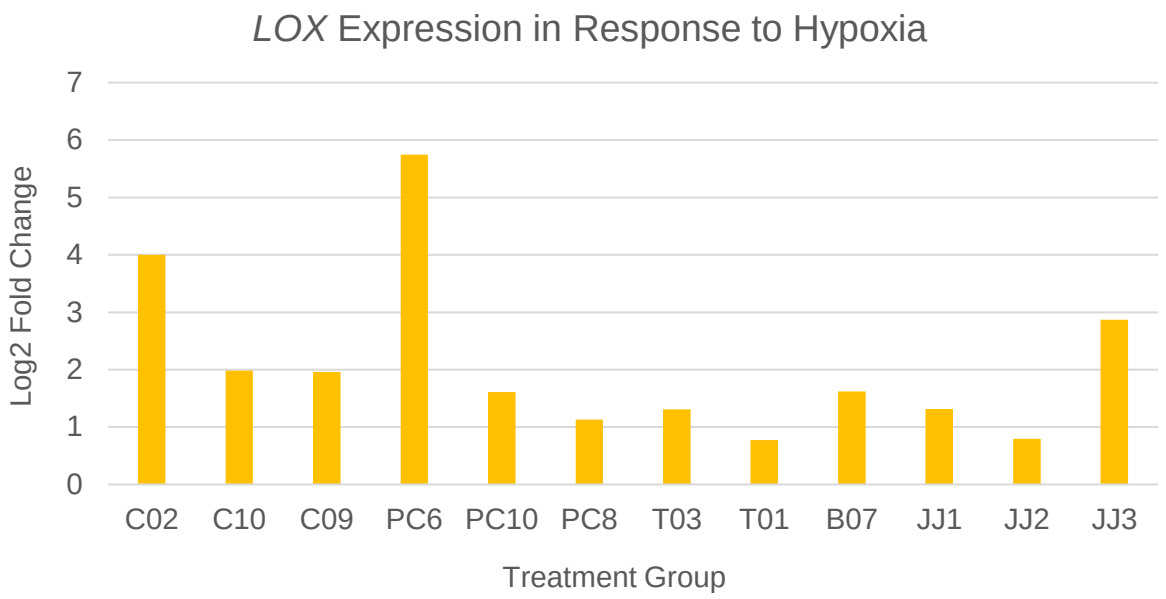

Figure 10. *LOX* Expression in Response to Hypoxia
The log2 fold change in *LOX* expression is shown for each patient sample incubated in hypoxic conditions compared to samples incubated in normoxic conditions. All samples upregulated *LOX* expression in response to chronic hypoxia after 24 hours of incubation at 5% oxygen and 95% nitrogen.

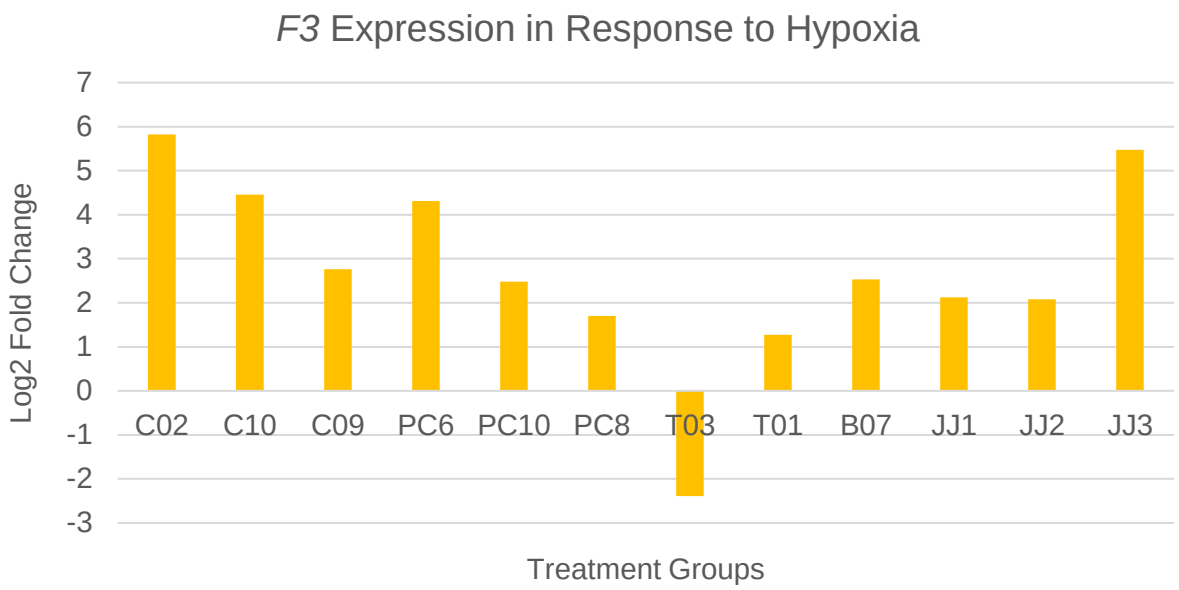

Figure 11. *F3* Expression in Response to Hypoxia
The log2 fold change in *F3* expression is shown for each patient sample incubated in hypoxic conditions compared to samples incubated in normoxic conditions. All samples upregulated *F3* expression in response to chronic hypoxia after 24 hours of incubation at 5% oxygen and 95% nitrogen, apart from one pectus excavatum patient, patient T03.

3.5 Combined Chronic Hypoxia and Transient Acidosis Slightly Diminishes the Effects of Hypoxia

Cultures exposed to chronic hypoxia (5% oxygen) for 24 hours and temporary acidosis at pH 5.5 for 60 seconds showed slight downregulation of *F3* and *LOX* compared to cultures subjected to hypoxia alone. On average across all three patient samples, control cultures downregulated *F3* -0.58-fold, PC samples downregulated *F3* -0.57-fold, PE samples downregulated *F3* -0.50-fold, and JJ012 samples downregulated *F3* -3.69-fold compared to cultures subjected to just hypoxia (Figure 12). *LOX* expression was also slightly downregulated across all cell types in response to combined hypoxia and acidosis compared to only hypoxia. On average across all three patient samples, control samples downregulated *LOX* -0.56-fold, PC samples downregulated *LOX* -0.55-fold, PE samples downregulated *LOX* -0.59-fold, and JJ012 samples downregulated *LOX* -2.24-fold compared to cultures subjected to just hypoxia (Figure 13). However, none of these results from either *F3* or *LOX* were significantly different

from the hypoxia response samples indicating that the hypoxia response on slightly lessened in the presence of hypoxia and acidosis.

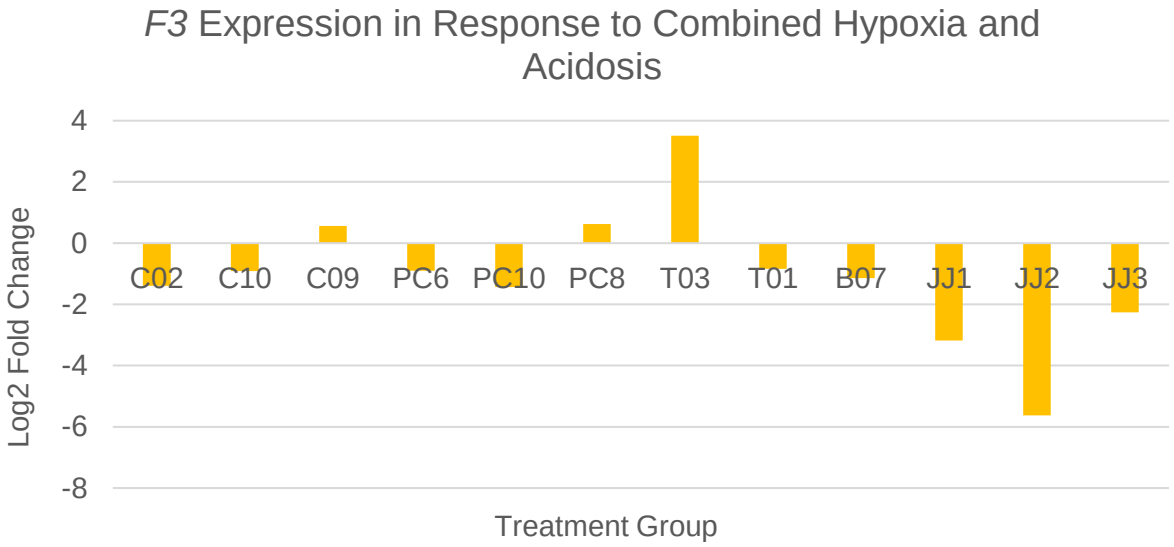

Figure 12. *F3* Expression in Response to Combined Hypoxia and Acidosis Compared to Hypoxia Alone
The log2 fold change in *F3* expression is shown for each patient sample exposed to combined chronic hypoxia (5% oxygen for 24-hour incubation) and temporary acidosis (pH 5.5 for 60 seconds) compared to samples exposed to chronic hypoxia alone. On average, none of these samples showed significant change between comparisons. However, note the larger fold change among JJ012 samples. This higher downregulation of *F3* in response to the combined hypoxia and acidosis requires further study as a potential marker for disease in chondrosarcoma. One patient sample from each cell type (C09, PC8, T03=PE) except JJ012 showed a slight upregulation of expression. Further investigation into other patient samples is required to explain these samples.

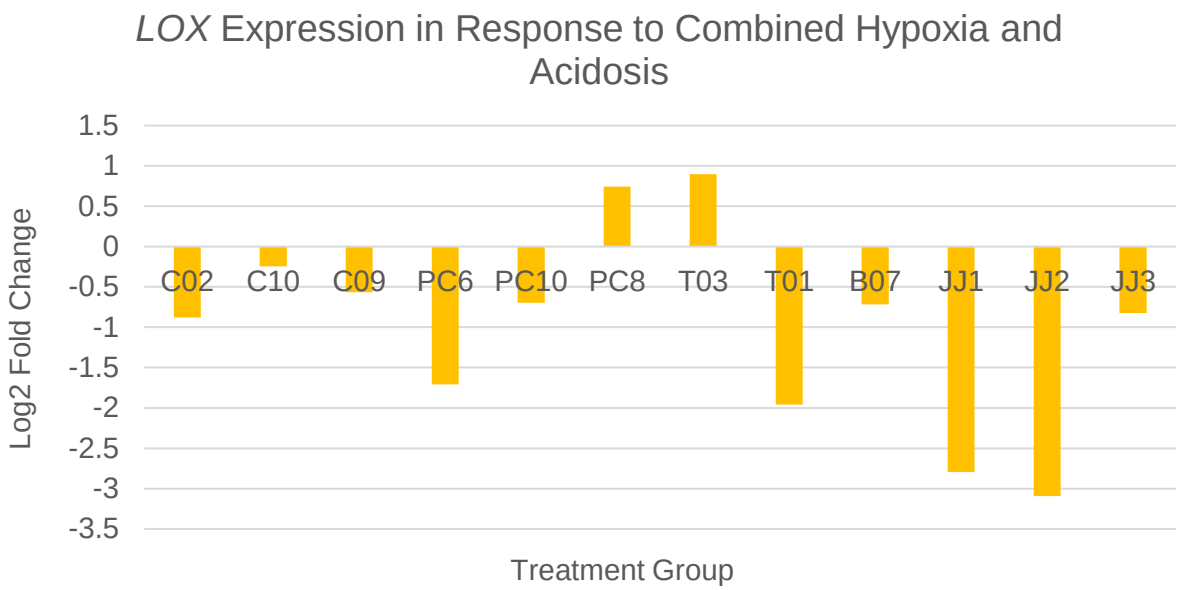

Figure 13. *LOX* Expression in Response to Combined Hypoxia and Acidosis Compared to Hypoxia Alone
The log2 fold change in *LOX* expression is shown for each patient sample exposed to combined chronic hypoxia (5% oxygen for 24-hour incubation) and temporary acidosis (pH 5.5 for 60 seconds) compared to samples exposed to chronic hypoxia alone. On average, none of these samples showed significant change between comparisons. However, note the larger fold change among JJ012 samples. This higher downregulation of *LOX* in response to the combined hypoxia and acidosis requires further study as a potential marker for disease in chondrosarcoma. Two patient samples, PC8 and T03 (PE), showed slight upregulation of *LOX*. Further study of other patient samples is required to explain this difference.

3.6 Gene Expression of F3 and LOX Significantly Differs Between Cell Types

F3 and *LOX* expression significantly varied between control costal cartilage, PC, PE, and JJ012 samples between all treatment groups (*LOX* p=0.0266, *F3* p=0.0370). These results indicate that each treatment group in each sample had different expression for both genes of interest. However, a post-hoc Tukey's Test for cell type showed no significant difference in overall expression between any of the diseased cartilage samples compared to the control (Tables 2 and 3).

Table 2. Post-hoc Tukey's Test for Cell Type in *F3*

Contrast	Estimate	Standard Error	Degrees of Freedom	T ratio	P value
Control:JJ012	0.7643960	0.9221174	25	0.829	0.8402
Control:PC	1.3413224	0.9221174	25	1.455	0.4787
Control:PE	-0.9700159	1.1293585	25	-0.859	0.8257
JJ012:PC	0.5769264	1.3040709	25	0.442	0.9705
JJ012:PE	-1.7344119	0.6520354	25	-2.660	0.0606
PC:PE	-2.3113383	1.4579956	25	-1.585	0.4048

A post-hoc Tukey's Test indicated no significant change in *F3* expression between diseased cartilages compared to the control.

Table 3. Post-hoc Tukey's Test for Cell Type in *LOX*

Contrast	Estimate	Standard Error	Degrees of Freedom	T ratio	P Value
Control:JJ012	0.9444082	0.6798596	25	1.389	0.5175
Control:PC	1.7704891	0.6798596	25	2.604	0.0682
Control:PE	0.2349261	0.8326545	25	0.282	0.9920
JJ012:PC	0.8260809	0.9614666	25	0.859	0.8255
JJ012:PE	-0.7094821	0.4807333	25	-1.476	0.4664
PC:PE	-1.5355630	1.0749524	25	-1.428	0.4941

A post-hoc Tukey's Test indicated no significant change in *LOX* expression between diseased cartilages compared to the control.

3.7 *F3* ANOVA

The results from the Three Factor ANOVA showed significant change in gene expression for *F3* between cell type (p=0.03700), oxygen levels (p=2.02e-06), and the interaction between cell type and oxygen levels (p=0.00998) (Table 4). However, the pairwise differences of contrast revealed the only valid comparisons that were significant were among treatment groups within the same cell type. Control cultures grown in hypoxia showed a significant upregulation (p=0.0001) in transcription levels of the *F3* gene compared to cultures grown in normoxia, but pH levels had no significant effect on *F3* expression. PC cultures showed similar results. The PC cultures grown under hypoxic conditions showed significant upregulation (p=0.0026) in

transcription levels of the *F3* gene compared to cultures grown in normoxia, but pH levels had no significant effect (Table 5). An error statistic was added to the ANOVA for patient variability and was found to be not significant. A post-hoc Tukey's test for cell type and oxygen levels was performed to determine that control and PC samples had significant difference in gene expression under hypoxic conditions (Table 6).

Table 4. *F3* Three Factor ANOVA Results

Factors Tested	Degrees of Freedom	Sum of Squares	Mean Square	F Value	P Value	Significance level *, **,***
Cell Type	3	16.80	5.60	3.293	0.03700	*
Oxygen levels	1	64.16	64.16	37.730	2.02e-06	***
pH	1	5.51	5.51	3.241	0.08389	
Cell Type * Oxygen Levels	3	23.86	7.95	4.677	0.00998	*
Cell Type * pH	3	8.08	2.69	1.583	0.21834	
Oxygen Levels * pH	1	1.98	1.98	1.163	0.29110	
Cell Type * Oxygen Levels * pH	3	7.48	2.49	1.466	0.24774	

The results from the three factor ANOVA show significant difference among cell type, oxygen levels, and the interaction between cell type and oxygen levels.

Table 5. Post-hoc Tukey's Test for Cell Type and Oxygen Levels in *F3* Expression

Contrast	Estimate	Standard Error	Degrees of Freedom	T ratio	P value
H,C - N,C	-4.49314	0.752906	25	-5.968	0.0001
H,C - H,JJ	-0.73041	1.064769	25	-0.686	0.9967
H,C - N,JJ	-2.23393	1.064769	25	-2.098	0.4427
H,C - H,PC	0.355556	1.064769	25	0.334	1
H,C - N,PC	-2.16605	1.064769	25	-2.034	0.4806
H,C - H,PE	-2.85102	1.248553	25	-2.283	0.3405
H,C - N,PE	-3.58215	1.248553	25	-2.869	0.1224
N,C - H,JJ	3.762722	1.064769	25	3.534	0.0297
N,C - N,JJ	2.259206	1.064769	25	2.122	0.4289
N,C - H,PC	4.848692	1.064769	25	4.554	0.0026
N,C - N,PC	2.327089	1.064769	25	2.186	0.3928
N,C - H,PE	1.642119	1.248553	25	1.315	0.8845
N,C - N,PE	0.910985	1.248553	25	0.73	0.9951
H,JJ - N,JJ	-1.50352	0.752906	25	-1.997	0.5033
H,JJ - H,PC	1.08597	1.408558	25	0.771	0.9932
H,JJ - N,PC	-1.43563	1.408558	25	-1.019	0.967
H,JJ - H,PE	-2.1206	0.841774	25	-2.519	0.233
H,JJ - N,PE	-2.85174	0.841774	25	-3.388	0.0412
N,JJ - H,PC	2.589486	1.408558	25	1.838	0.6018
N,JJ - N,PC	0.067883	1.408558	25	0.048	1
N,JJ - H,PE	-0.61709	0.841774	25	-0.733	0.995
N,JJ - N,PE	-1.34822	0.841774	25	-1.602	0.745
H,PC - N,PC	-2.5216	0.752906	25	-3.349	0.0449
H,PC - H,PE	-3.20657	1.552155	25	-2.066	0.4617
H,PC - N,PE	-3.93771	1.552155	25	-2.537	0.226
N,PC - H,PE	-0.68497	1.552155	25	-0.441	0.9998
N,PC - N,PE	-1.4161	1.552155	25	-0.912	0.982
H,PE - N,PE	-0.73113	0.752906	25	-0.971	0.9745

Not all comparisons are valid, but significant difference is shown among control samples and among PC samples.

Legend: Cell Types- C=Control, PC=Pectus Carinatum, PE=Pectus Excavatum, JJ=JJ012
Oxygen levels- N=normoxia, H=hypoxia

3.8 *LOX* ANOVA

The results from the Three Factor ANOVA showed significant change in gene expression for *LOX* between cell type (p=0.0266), oxygen levels (p=1.81e-06), pH (p=0.0368), and the interaction between cell type and oxygen level (p=0.0323). However, the pairwise differences of contrast revealed the only valid comparisons that were significant were among treatment groups within the same cell type. Like *F3* expression, *LOX* expression levels were significantly upregulated in response to hypoxia compared to normoxia within the control cultures (p=0.0009) and within the PC cultures (p=0.0047), but pH had no significant effect (Table 6). An error statistic was added to the ANOVA for patient variability and was found to be not significant. A post-hoc Tukey's test for cell type and oxygen levels was performed to determine that control and PC samples had significant difference in gene expression under hypoxic conditions (Table 7).

Table 6. *LOX* Three Factor ANOVA Results

Factors Tested	Degrees of Freedom	Sum of Squares	Mean Square	F Value	P Value	Significance Level: *,**,***
Cell Type	3	10.07	3.36	3.630	0.0266	*
Oxygen Levels	1	35.37	35.37	38.265	1.81e-06	***
pH	1	4.50	4.50	4.867	0.0368	*
Cell Type*Oxygen Levels	3	9.51	3.17	3.430	0.0323	*
Cell Type*pH	3	5.42	1.81	1.955	0.1466	
Oxygen Levels*pH	1	1.68	1.68	1.821	0.1893	
Cell Type*Oxygen Levels*pH	3	1.03	0.34	0.371	0.7745	

The results from the three factor ANOVA show significant difference between cell types, oxygen levels, pH, and the interaction between cell type and oxygen levels.

Table 7. Post-hoc Tukey's Test for Cell Type and Oxygen Levels in *LOX* Expression

Contrast	Estimate	Standard Error	Degrees of Freedom	T ratio	P Value
C,H - JJ,H	0.112389	0.785034	25	0.143	1
C,H - PC,H	1.584909	0.785034	25	2.019	0.4899
C,H - PE,H	-0.84473	0.920534	25	-0.918	0.9814
C,H - C,N	-2.76553	0.555103	25	-4.982	0.0009*
C,H - JJ,N	-0.9891	0.785034	25	-1.26	0.9049
C,H - PC,N	-0.80946	0.785034	25	-1.031	0.9649
C,H - PE,N	-1.45094	0.920534	25	-1.576	0.7594
JJ,H - PC,H	1.47252	1.038503	25	1.418	0.8406
JJ,H - PE,H	-0.95712	0.620624	25	-1.542	0.778
JJ,H - C,N	-2.87791	0.785034	25	-3.666	0.0219*
JJ,H - JJ,N	-1.10149	0.555103	25	-1.984	0.511
JJ,H - PC,N	-0.92184	1.038503	25	-0.888	0.9846
JJ,H - PE,N	-1.56333	0.620624	25	-2.519	0.2331
PC,H - PE,H	-2.42964	1.144374	25	-2.123	0.4281
PC,H - C,N	-4.35043	0.785034	25	-5.542	0.0002
PC,H - JJ,N	-2.57401	1.038503	25	-2.479	0.2496
PC,H - PC,N	-2.39436	0.555103	25	-4.313	0.0047
PC,H - PE,N	-3.03585	1.144374	25	-2.653	0.1841
PE,H - C,N	-1.92079	0.920534	25	-2.087	0.4494
PE,H - JJ,N	-0.14436	0.620624	25	-0.233	1
PE,H - PC,N	0.035277	1.144374	25	0.031	1
PE,H - PE,N	-0.60621	0.555103	25	-1.092	0.9526
C,N - JJ,N	1.776428	0.785034	25	2.263	0.3512
C,N - PC,N	1.95607	0.785034	25	2.492	0.2441
C,N - PE,N	1.314584	0.920534	25	1.428	0.8359
JJ,N - PC,N	0.179642	1.038503	25	0.173	1
JJ,N - PE,N	-0.46184	0.620624	25	-0.744	0.9945
PC,N - PE,N	-0.64149	1.144374	25	-0.561	0.9991

Not all comparisons are valid, but significant difference is shown among control samples and among PC samples.

Legend: Cell Types- C=Control, PC=Pectus Carinatum, PE=Pectus Excavatum, JJ=JJ012
Oxygen levels- N=normoxia, H=hypoxia

CHAPTER 4

DISCUSSION

The results from this study opened doors to many possibilities in the future and helped to gain insight on how chondrocytes respond to natural stimuli like low oxygen levels and low pH. Due to limited funds and difficulties in obtaining control samples of costal cartilage, only 3 replicates were completed for each treatment group. More replicates to increase the sample size would add more power to the analysis and minimize error due to possible patient variability. Variability among cells taken from the same patient must also be considered for further studies with single cells, such as the real-time analysis of intracellular calcium transit.

Results from the ANOVA table showed significant change in *LOX* and *F3* expression in response to hypoxia, but no significant change in expression in response to combined hypoxia and acidosis. On average *LOX* expression was upregulated in both hypoxia and combined hypoxia and acidosis in both control and PC groups. However, fold changes were slightly larger in cultures grown under hypoxia at neutral pH compared to those grown under hypoxia combined with acidosis. This suggests that combined hypoxia and acidosis slightly diminish the effects of hypoxia, but still trigger a change in expression. Additional study of these combined effects in chondrocytes only cements the notion that studies performed on chondrocytes grown in normoxic and neutral pH conditions is not comparable to *in vivo* studies.

LOX and *F3* were significantly upregulated at the transcriptional level in the control and PC samples, but not in the JJ012 or PE samples. Healthy costal cartilage may respond to changing oxygen levels whereas the diseased cartilage doesn't due to a malfunction in the hypoxia response pathway. My results indicate that the normal response to hypoxic conditions in chondrocytes may be to upregulate transcription of *F3* and *LOX* to increase the chances of preventing NO mediated apoptosis and increase the structural integrity of the cartilage due to more crosslinked collagen fibers (Zhang et al., 2017; Zhong et al., 2008). Protein analysis would test this hypothesis and determine if any post-translational modification changes the protein expression. However, PC samples showed upregulation of *LOX* and *F3* as well as the control. This response may be an indication of a separate response to hypoxia from the PE samples and could be used as a possible biomarker for PC patients with further study.

Further melt curve analysis of theoretical versus experimental melting temperatures of each gene of interest could determine the possibility of SNPs (Single Nucleotide Polymorphisms) for

F3 and *LOX* genes within each cell type. Detection of these SNPs could open a new avenue of potential mutations within pectus deformities and chondrosarcoma.

Preliminary data from our calcium transit experiments showed a marked change in response to extracellular acidosis, but our gene expression analysis of the hypoxia response pathway did not show any significant changes due to pH. These contrasting results could possibly be explained by possible change in the hypoxia pathway over time. In the hypoxia pathway, HIF-1A is the master regulator as a transcription factor with a large amount of target genes. In gastric cancer, HIF-1A regulates the expression of ADM (Adrenomedullin) and VEGFA (Vascular Endothelial Growth Factor A) in early stages of hypoxia, through 6 hours after exposure. However, HIF-1A expression dropped and a second regulator, NDRG3, peaked after 24 hours of exposure (Qiao et al., 2017). Our cells were cultured in 5% oxygen for 24 hours prior to RNA extraction. The possibility of the hypoxia response and probably the response to low pH may change over time. For future experiments, I suggest growing cells in treatment for less time and to use a low pH media for the entirety of the incubation period instead of performing the RNA extraction after 60 seconds of exposure to low pH.

Malfunctions with acid-sensitive ion channels (ASICs) involved with intracellular calcium transit could be used as a model for potential disease mechanism in chest wall deformities and chondrosarcoma. In a model with mouse ventricular cardiomyocytes, ASICs such as OGR1 accept protons and stimulate internal stores to transit calcium into the cytoplasm under acidic conditions which subsequently causes an upregulation of HIF-1α (Figure 14) (Hu et al., 2017). Activated by HIF-1α, Sox5 and Sox9 work as transcription factors that have major roles in stimulating chondrocyte differentiation and suppressing apoptosis respectively (Akiyama et al., 2002). Preliminary gene expression data shows a downregulation of *Sox5* and *Sox9* genes and an upregulation of *OGR1* in response to low pH in chondrosarcoma cell line JJ012. The combined response of intracellular calcium transit and ASICs to chronic hypoxia and transient acidosis is not fully understood and could open potential avenues of research in cartilage biology.

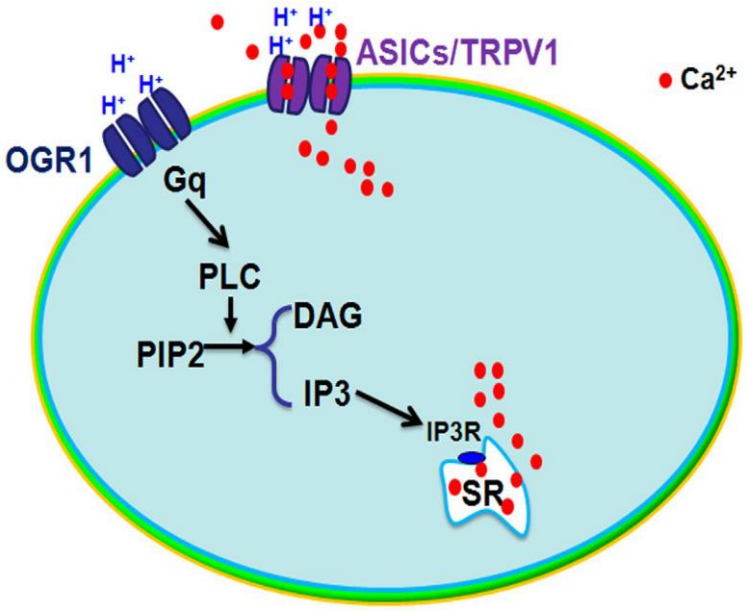

Figure 14. Acid-Sensitive Ion Channels in Rat Cardiomyocytes
ASICs in rat cardiomyocytes respond to extracellular acidosis by accepting protons and stimulating intracellular calcium transit from the sarcoplasmic reticulum into the cytoplasm (Hu et al., 2017).

Due to increased glycolytic metabolism and cell signaling pathways involved in the production of NO, Reactive Oxygen Species (ROS) and Reactive Nitrogen Species (RNS) accumulate in abundance within the mitochondria and eventually in the ECM. In the hypoxia response pathway, ROS and RNS lead to cell death through downstream effects. In a study conducted on cortical neurons, mitochondrial morphology changed due to oxygen level and low pH. In the presence of low oxygen, the mitochondria began to fracture and undergo fission. The addition of mild levels of extracellular acidosis (pH 6.5 and above) reversed the fission and inhibited mitochondrial fracturing (Khacho et al., 2014). Here we see a response at the source of glycolytic metabolism to external stressors. To further investigate these effects, I suggest that the mitochondria of cell cultures exposed to hypoxia and acidosis should be imaged through Transmission Electron Microscopy. Observation of the mitochondrial response will allow for new insight into how chondrocytes cope with their unforgiving surroundings.

At the beginning of our experimental design process, we chose to include pectus excavatum sample PE44 due to multiple corrective surgeries with poor outcome. However, the isolated cells did not proliferate in culture very well. After three weeks in monolayer culture, the culture was only ~60% confluent. Upon observation every few days, the cells appeared to die just as quickly as they proliferated leading to no increase in total number. This sample would have been an interesting addition to our data, but not enough cells were grown to split into enough cultures for all four experimental conditions.

CHAPTER 5

CONCLUSIONS

In conclusion, hypoxic conditions markedly increased expression levels of the *F3* and *LOX* genes within the control group and PC group, but not in the chondrosarcoma cell line or PE samples. Pending supporting protein analysis, these results suggest the normal physiological response in chondrocytes to hypoxia is to increase the production of F3 to prevent NO mediated apoptosis, and LOX to enhance cartilage strength through LOX mediated collagen crosslinking. Acidosis had no significant effect on *F3* expression, but *LOX* expression was slightly upregulated in cultures exposed to transient acidosis. Combined chronic hypoxia and temporary acidosis appears to slightly diminish the increased expression found in cultures grown under hypoxic conditions alone. A more comprehensive investigation into how chondrocytes respond to their natural oxidative stress and acidic extracellular environment will further the field of cartilage biology and possibly change the way experiments are conducted in laboratories.

REFERENCES

Akiyama, H., Chaboissier, M.-C., Martin, J.F., Schedl, A., and de Crombrugghe, B. (2002). The transcription factor Sox9 has essential roles in successive steps of the chondrocyte differentiation pathway and is required for expression of *Sox5* and *Sox6*. Genes Dev *16*, 2813-2828.

Alice, J.S.F., Asheesh, B., and Scott, A.R. (2009). The Basic Science of Articular Cartilage: Structure, Composition, and Function. Sports Health *1*, 461-468.

Asmar, A., Barrett-Jolley, R., Werner, A., Kelly, R., and Stacey, M. (2016). Membrane channel gene expression in human costal and articular chondrocytes. Organogenesis *12*, 94-107.

Asmar, A., Werner, A., Kelly Jr, R., Fecteau, A., and Stacey, M.W. (2015). Presence and Localization of Pro-and Mature Forms of Biglycan and Decorin in Human Costal Cartilage Derived from Chest Wall Deformities. AJMD *2*, 1012.

CoreTeam, R. (2013). R: A Language and Environment for Statistical Computing.

Creswick, H.A., Stacey, M.W., Kelly, R.E., Gustin, T., Nuss, D., Harvey, H., Goretsky, M.J., Vasser, E., Welch, J.C., Mitchell, K.*, et al.* (2006). Family study of the inheritance of pectus excavatum. J Pediatr Surg *41*, 1699-1703.

de Barros, C.N., Miluzzi Yamada, A.L., Junior, R.S.F., Barraviera, B., Hussni, C.A., de Souza, J.B., Watanabe, M.J., Rodrigues, C.A., and Garcia Alves, A.L. (2016). A new heterologous fibrin sealant as a scaffold to cartilage repair—Experimental study and preliminary results. Exp Biol Med *241*, 1410-1415.

Dean, C., Etienne, D., Hindson, D., Matusz, P., and Tubbs, S.R. (2012). Pectus excavatum (funnel chest): a historical and current prospective. SRA *34*, 573-579.

Dudhia, J. (2005). Aggrecan, Aging, and Assembly in Articular Cartilage. CMLS *62*, 2241-2256.

Genecards.org (2018a). F3 gene. In Genecards, Weizmann Institute of Science. http://www.genecards.org/cgi-bin/carddisp.pl?gene=F3

Genecards.org (2018b). LOX gene. In Genecards, Weizmann Institute of Science. http://www.genecards.org/cgi-bin/carddisp.pl?gene=LOX&keywords=LOX

Goretsky, M.J., Kelly Re Jr Fau - Croitoru, D., Croitoru D Fau - Nuss, D., and Nuss, D. (2004). Chest wall anomalies: pectus excavatum and pectus carinatum. Adolesc Med *15*, 455-471.

Horth, L., Stacey, M., Benjamin, T., Segna, K., Proud, V., Nuss, D., and Kelly, R. (2012). Genetic analysis of inheritance of pectus excavatum. J Pediatr Genet *1*, 161-173.

Hu, Y.-L., Mi, X., Huang, C., Wang, H.-F., Song, J.-R., Shu, Q., Ni, L., Chen, J.-G., Wang, F., and Hu, Z.-L. (2017). Multiple H+ sensors mediate the extracellular acidification-induced [Ca2+]i elevation in cultured rat ventricular cardiomyocytes. Sci Rep *7*, 44951.

Huwe, L., Brown, W., Hu, J., and Athanasiou, K. (2017a). Characterization of costal cartilage and its suitability as a cell source for articular cartilage tissue engineering J Tissue Eng Regen Med *[Epub ahead of print]*.

Huwe, L.W., Sullan, G.K., Hu, J.C., and Athanasiou, K.A. (2017b). Using Costal Chondrocytes to Engineer Articular Cartilage with Applications of Passive Axial Compression and Bioactive Stimuli. Tissue Engineering Part A *24*, 516-526.

Jeong, W., and Kim, H.-J. (2018). Biomarkers of chondrosarcoma. Journal of Clinical Pathology [Epub ahead of print].

Kanehisa, M., Furumichi, M., Tanabe, M., Sato, Y., and Morishima, K. (2017). KEGG: new perspectives on genomes, pathways, diseases and drugs. Nucleic Acids Res *45*, D353-D361.

Kanehisa, M., and Goto, S. (2000). KEGG: Kyoto Encyclopedia of Genes and Genomes. Nucleic Acids Res *28*, 27-30.

Kanehisa, M., Sato, Y., Kawashima, M., Furumichi, M., and Tanabe, M. (2016). KEGG as a reference resource for gene and protein annotation. Nucleic Acids Res *44*, D457-D462.

Khacho, M., Tarabay, M., Patten, D., Khacho, P., MacLaurin, J.G., Guadagno, J., Bergeron, R., Cregan, S.P., Harper, M.-E., Park, D.S.*, et al.* (2014). Acidosis overrides oxygen deprivation to maintain mitochondrial function and cell survival. Nat Commun *5*, 3550.

Kiani, C., Chen, L., Wu, Y.J., Yee, A.J., and Yang, B.B. (2002). Structure and function of aggrecan. Cell Res *12*, 19.

Koumbourlis, A.C., and Stolar, C.J. (2004). Lung growth and function in children and adolescents with idiopathic pectus excavatum. Pediatr Pulmonol *38*, 339-343.

Licari, L.G., and Kovacic, J.P. (2009). Thrombin physiology and pathophysiology. J Vet Emerg Crit Care (San Antonio) *19*, 11-22.

Nuss, D., and Kelly, R.E. (2010). Indications and Technique of Nuss Procedure for Pectus Excavatum. Thorac Surg Clin *20*, 583-597.

Qiao, F., Fang, J., Xu, J., Zhao, W., Ni, Y., Akuo, B.A., Zhang, W., Liu, Y., Ding, F., Li, G.*, et al.* (2017). The role of adrenomedullin in the pathogenesis of gastric cancer. Oncotarget *8*, 88464-88474.

Shen, J., Stacey, M.W., and Hao, Z. (2018). A distributed-deflection sensor with a built-in probe for conformal mechanical measurements of costal cartilage at its exterior surface. IEEE Sensors *18*, 822-829.

Stacey, M., Dutta, D., Cao, W., Asmar, A., Elsayed-Ali, H., Kelly, R., and Beskok, A. (2013). Atomic force microscopy characterization of collagen 'nanostraws' in human costal cartilage. Micron *44*, 483-487.

Stacey, M.W., Grubbs, J., Asmar, A., Pryor, J., Elsayed-Ali, H., Cao, W., Beskok, A., Dutta, D., Darby, D.A., Fecteau, A.*, et al.* (2012). Decorin Expression, Straw-like Structure, and Differentiation of Human Costal Cartilage. Con Tissue Res *53*, 415-421.

Wikipedia (2018a). Pectus Carinatum. In Wikipedia, the Wikimedia Foundation Inc.. https://en.wikipedia.org/wiki/Pectus_carinatum

Wikipedia (2018b). Pectus Excavatum. In Wikipedia, the Wikimedia Foundation Inc.. https://en.wikipedia.org/wiki/Pectus_excavatum

Williams, A.M., and Crabbe, D.C.G. (2003). Pectus deformities of the anterior chest wall. Ped Resp Rev *4*, 237-242.

Yuan, F.-L., Wang, H.-R., Zhao, M.-D., Yuan, W., Cao, L., Duan, P.-G., Jiang, Y.-Q., Li, X.-L., and Dong, J. (2014). Ovarian Cancer G protein-Coupled Receptor 1 Is Involved in Acid-Induced Apoptosis of Endplate Chondrocytes in Intervertebral Discs. J Bone Miner Res *29*, 67-77.

Zhang, Y., Morgan, B.J., Smith, R., Fellows, C.R., Thornton, C., Snow, M., Francis, L.W., and Khan, I.M. (2017). Platelet-rich plasma induces post-natal maturation of immature articular cartilage and correlates with LOXL1 activation. Sci Rep *7*, 3699.

Zhong, M., Wike, L.J., Ryaby, J.T., Carney, D.H., Boyan, B.D., and Schwartz, Z. (2008). Thrombin peptide TP508 prevents nitric oxide mediated apoptosis in chondrocytes in the endochondral developmental pathway. Biochim Biophys Acta *1783*, 12-22.

VITA

Jamie L. Durbin

Department of Biological Sciences

Old Dominion University

Norfolk, VA 23529

Education

- Bachelor of Science in Biology

  Old Dominion University, May 2014

- Master of Science in Biology

  Old Dominion University, May 2018

Teaching/Research Experience

- Teaching Assistant: Gross Anatomy/ Cadaver Dissection Physical Therapy Program
  May 2014-July 2014
  Department of Biology, Old Dominion University

- Graduate Teaching Assistant: Anatomy and Physiology Laboratory BIOL 250/251
  August 2017-May 2018
  Department of Biology, Old Dominion University

Presentations

- Old Dominion University Biology Graduate Student Spring Symposium, “Plastinates in the Undergraduate Anatomy Lab”, April 2017

- ISBioTech Spring Conference for Bioprocessing Technologies, Poster, “Plastinates In the Anatomy Lab: A Safe Alternative to Formalin Fixed Tissue”, March 2018